

Systematics in the electron spectrum measured by ATIC

A. D. Panov*, V. I. Zatsepin*, N. V. Sokolskaya*, J. H. Adams, Jr.[†], H. S. Ahn[‡]
 G. L. Bashindzhagyan*, J. Chang[§], M. Christl[†], T. G. Guzik[¶], J. Isbert[¶],
 K. C. Kim[‡], E. N. Kouznetsov*, M. I. Panasyuk*, E. B. Postnikov*, E. S. Seo[‡],
 J. Watts[†], J. P. Wefel[¶], and J. Wu[‡]

*Skobeltsyn Institute of Nuclear Physics, Moscow State University, Moscow, Russia

[†]Marshall Space Flight Center, Huntsville, AL, USA

[‡]University of Maryland, Institute for Physical Science & Technology, College Park, MD, USA

[§]Purple Mountain Observatory, Chinese Academy of Sciences, China

[¶]Louisiana State University, Department of Physics and Astronomy, Baton Rouge, LA, USA

Abstract. An analysis of different parameters to separate electrons from protons in the ATIC experiment has been performed. Five separate discriminants were studied by different Monte Carlo programs, leading to a variety of results. Application to the ATIC data indicates the range of variation possible in the interpretation of the data. The results of this analysis, when compared with the published results [5], show good agreement in the most interesting region of energy (from 90 GeV to 600 GeV). The measured electron spectrum is compared with the recent data reported by Fermi/LAT, and there is no major disagreement between ATIC's results and Fermi/LAT. Finally, possible systematics-free, short energy scale features of the ATIC electron spectrum are mentioned.

Keywords: ATIC, electron spectrum, fine structure

The ATIC (Advanced Thin Ionization Calorimeter) balloon-borne spectrometer was designed to measure the energy spectra of elements from H to Fe with individual resolution of charges in primary cosmic rays for energy region from 50 GeV to 100 TeV. ATIC had three successful flights around the South Pole from the station McMurdo in 2000–2001 (ATIC-1), 2002–2003 (ATIC-2) and 2007–2008 (ATIC-4). ATIC is comprised of a fully active bismuth germanate (BGO) calorimeter, a carbon target with embedded scintillator hodoscopes, and a silicon matrix that is used as the main charge detector. The calorimeter is comprised of 8 layers with 40 BGO crystals in each for ATIC-1 and ATIC-2 and of 10 layers for ATIC-4. The details of the construction of the apparatus and the procedures of its calibration are described in the papers [1], [2], [3], [10]. It was shown that it is possible also to measure the spectrum of cosmic ray electrons plus positrons [4] with ATIC (hereinafter we use 'electrons' for brevity). To separate electrons from the higher background of protons and other nuclei differences in shower development for incident electrons and for nuclei are used, guided by measured quantities such as secondary gamma rays, accelerator calibrations and simulations [6]. The spectrum of electrons measured

with the ATIC spectrometer by this method was published in the paper [5]. The most notable detail of the electron spectrum reported was an 'excess' of electrons between energies of 300–800 GeV. The main purpose of this report is to investigate possible alternate techniques to separate electrons from hadrons based solely upon currently available simulation methodologies. This analysis was carried out completely independent of the previous analysis, starting from the low level procedures of the calibration of the ATIC apparatus (except the calibration of the silicon matrix detector) and analyzing the data with the new discriminants to look at the resulting electron spectrum. Note that all the lines of reasoning and final conclusions of the present work do not comply exactly with techniques of the papers [4], [5] but rather presents an approach, and its implications, for further discussion. We should note also that the results of the present work are preliminary since the work is still in progress.

To describe the shape of the shower in the calorimeter the following parameters were used in [5]. The first two parameters are C_l – relative energy deposit in the l -th layer ($l = 0, 1, \dots$) of the calorimeter (cascade curve) and R_l – root mean square (RMS) of the energy deposited in l -th layer of the calorimeter

$$C_l = E_l/E_d, \quad R_l^2 = \frac{\sum_i E_l^i (X_i - X_l^c)^2}{\sum_i E_l^i}, \quad (1)$$

where E_d is the energy deposit in the calorimeter, E_l is the energy deposit in l -th layer, X_l^c is the center of weight for energy distribution in l -th layer, X_i is the coordinate of the i -th BGO in l -th layer, E_l^i is the energy deposit measured in this scintillator. Third parameter F_l was defined in [5] by $F_l = R_l^2 C_l$, where R_l is measured in millimeters. We instead introduce the parameter G_l defined by

$$G_l^2 = R_l^2 C_l. \quad (2)$$

To select electrons from proton background a special quantity that numerically (for R_l measured in mm and for F_l measured in mm^2) is

$$Ch = R_0 + R_1 + F_6 + F_7 \quad (3)$$

was used (together with a number of additional conditions) in the paper [5]. The shower for an electron event is narrower than for hadron events and Ch is some measure of the width of the shower. Therefore Ch could be used as an 'electron filter'. Some cut level Ch_0 should be defined to work with the filter: the events with $Ch < Ch_0$ selected as electrons and other ones as hadrons.

Our purpose was to carry out the analysis on the basis of other filters. To define filters, we used basic parameters C_l, R_l, G_l to describe shower development. For better cross-checking of the results we defined and worked with five new filters. Four filters (simple filters) were similar to the filter Ch but used 8 layers of the calorimeter:

$$\chi = \sqrt{\frac{1}{8} \left[\sum_{l=0}^3 \left(\frac{R_l - \bar{R}_l}{\sigma_l^R} \right)^2 + \sum_{l=4}^7 \left(\frac{G_l - \bar{G}_l}{\sigma_l^G} \right)^2 \right]} \quad (4)$$

$$R = \sqrt{\frac{1}{8} \left[\sum_{l=0}^3 \left(\frac{R_l - \bar{R}_l}{\bar{R}_l} \right)^2 + \sum_{l=4}^7 \left(\frac{G_l - \bar{G}_l}{\bar{G}_l} \right)^2 \right]} \quad (5)$$

$$L1 = \frac{1}{8} \left[\sum_{l=0}^3 \frac{R_l}{\bar{R}_l} + \sum_{l=4}^7 \frac{G_l}{\bar{G}_l} \right] \quad (6)$$

$$L2 = \sqrt{\frac{1}{8} \left[\sum_{l=0}^3 \left(\frac{R_l}{\bar{R}_l} \right)^2 + \sum_{l=4}^7 \left(\frac{G_l}{\bar{G}_l} \right)^2 \right]} \quad (7)$$

Here \bar{R}_l, \bar{G}_l are mean values for R_l, G_l simulated by FLUKA system¹ [7] (for some definite energy: all filters are energy dependent); σ_l^R, σ_l^G are mean simulated standard deviations for R_l, G_l from mean values \bar{R}_l, \bar{G}_l . The fifth filter was defined as

$$LogP = \log_{10} \left(\prod_{l=0}^7 P_l(E_d, C_l, R_l) \right) \quad (8)$$

where $P_l(E_d, C_l, R_l)$ are simulated for the incident isotropic electrons and then numerically tabulated against deposited energy E_d distributions of probability for the shower parameters C_l, R_l in l -th layer of the calorimeter. The filter $LogP$ has essentially other nature than the filters (4)–(7) and the filter Ch of [5]. It was appeared that each filter may be used separately but the best result (lower level of proton contamination with preserving of the electron events) is provided by simultaneous using of all five filters. This idea defines the sixth 'product filter'

$$J = \chi \times R \times L1 \times L2 \times LogP. \quad (9)$$

The order of the terms is unimportant in (9). The lowest background level for the filter J may be seen in Fig. 1. The main results of this work are obtained with the filter J .

The first conclusion obtained during analysis was that the procedure of the proton background subtraction

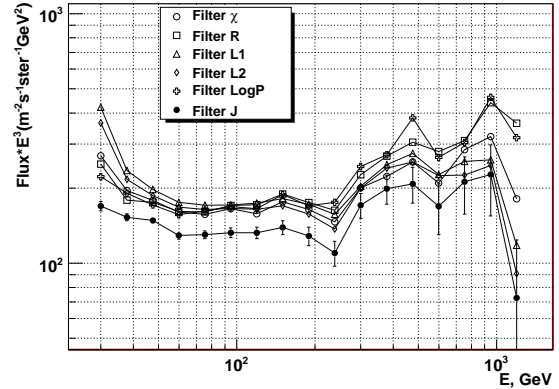


Fig. 1. The spectra of selected electron-like events for the ATIC-2 flight (electron spectra without background subtraction) obtained with the filters $\chi, R, L1, L2, LogP$ and with the 'product' filter J .

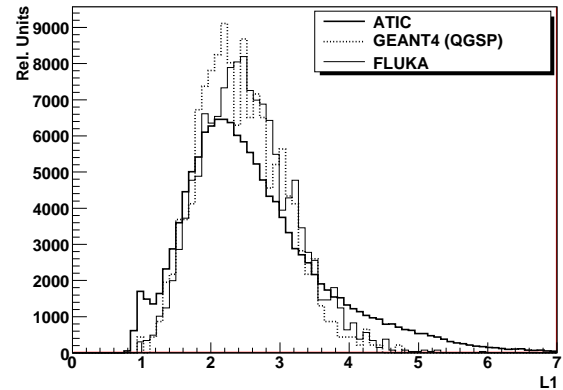


Fig. 2. Simulation of the response of the filter $L1$ for the protons with power spectrum with index -2.7 and the energy deposit between 50 GeV and 100 GeV by FLUKA and GEANT4 systems and the same measured in ATIC-2 experiment. All three plots do not agree with each other.

from the spectrum of the selected electron-like events, using purely simulations, may be a source of significant systematics. This conclusion is valid for all studied filters. The key point is that this problem is similar to an ill-defined problem. The proton background should be calculated by simulation of the protons cascades in the ATIC calorimeter (and other parts of the apparatus). Since the flux of the cosmic rays electrons is only a small fraction of the flux of the cosmic rays protons (from $\sim 1 \cdot 10^{-2}$ to less than $\sim 1 \cdot 10^{-3}$) then even small errors in the simulation of the protons cascades may lead to large errors in the estimation of the proton contamination of the electron spectrum. More over, we found that various simulation codes actually do not agree sufficiently well with each other and with the experiment in the simulation of the response of the electron filters. This is illustrated in Fig. 2 for FLUKA [7] and GEANT4 [8] codes (GEANT 4.9.1 was used). Further, we found that even for the same simulation code, different filters may produce drastically different results after subtraction of the calculated proton background. Therefore we should

¹The version is FLUKA 2008.3.

not rely solely upon the simulated proton background subtraction, but, instead, one should try to reduce the proton contamination as much as possible and utilize in-flight data as 'calibration' to the extent feasible. The things that may be safely studied are various features in the behavior of the electron spectrum (like 'ATIC's excess'). It is seen in Fig. 1 that the 'ATIC's excess' holds for each filter in spite of different background level for different filters.

The next issue is the problem of the accounting for the scattering of the electrons in the atmosphere which is not straightforward. The effective thickness of the atmosphere is approximately 8 kilometers and this distance is approximately the averaged distance between the point of emission of the secondary gammas by the electron and ATIC apparatus. The mean angle of the emitted quanta is $\phi \sim m_e c^2 / E_{prim}$. Therefore for energies of the electron from 50 GeV to 1000 GeV these angles are from 1×10^{-5} to 0.5×10^{-6} respectively. Such angles produce mean deviation of the quanta from the trajectory of the electron at the level of the apparatus of 10 cm (for 50 GeV) to 0.5 cm (for 1000 GeV). With high probability, such gammas will be detected by the calorimeter (square $50 \times 50 \text{ cm}^2$) together with the incident electron. Therefore, the loss of energy generally may be small or even negligible. But the side gammas may in some cases distort the shape of the 'standard' electron shower in the calorimeter and an electron filter may reject this event as a non-electron, leading to an inefficiency. But what is the probability of improperly rejecting electrons due to the side gammas? Generally, it is a difficult question. To answer it one should simulate exactly the atmospheric gammas, then using the simulation of the ATIC apparatus one should calculate the response to them and finally decide whether the whole cascade is registered as an electron by the filter or not. We have not resolved this issue up to now, but simply point to it as an area that is still under investigation. Note that for energies 500–1000 GeV the deviations of gammas from the electron are so small that they almost certainly do not prevent the classification the event as electron-like and the measured electron flux at the top of the apparatus and the flux at the top of the atmosphere would be the same. This requires a detailed Monte-Carlo investigation to confirm.

Now we would like to compare our calculated spectrum of electrons with the spectrum of the paper [5]. The problem is that the spectrum of [5] was corrected for the scattering of the electrons in the atmosphere by simple rescaling the energy of electrons. Therefore to compare the spectra we artificially normalize the energy of each event of our spectrum by factor 1.15 that corresponds to the mean loss of energy by the electrons in the atmosphere. The factor 1.15 is

$$\exp\left(-\frac{t}{\tau_{air}} \cos^2 \bar{\theta}\right) = \frac{1}{1.15},$$

where $t = 4.8 \text{ g/cm}^2$ is mean depth of the atmosphere

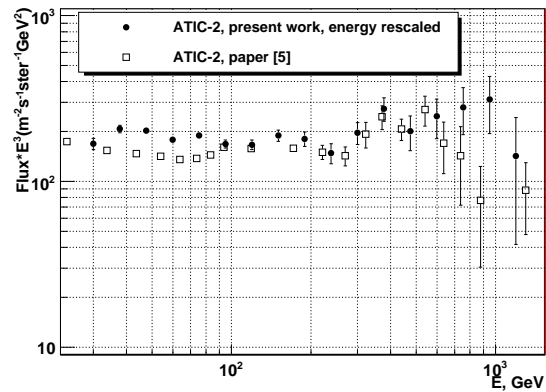


Fig. 3. Comparison of the electron spectrum of present paper (obtained with the filter J and with rescaling of the energy by the factor 1.15, see text for explanation) with the spectrum of the paper [5]. The background is subtracted in the spectrum of the paper [5] but is not subtracted in the spectrum of present paper.

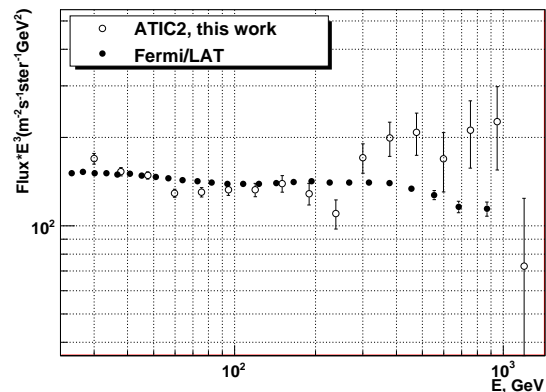


Fig. 4. Comparison of the electron spectrum of ATIC-2 (present paper, no background subtraction, no rescaling of energy) with the electron spectrum measured by Fermi/LAT [9].

during ATIC-2 flight, $\tau_{air} = 37.1 \text{ g/cm}^2$ is the radiation length for air and θ is mean zenith angle of the incident electron. The result of the comparison is shown in Fig. 3. It is seen that there exists very good agreement of both spectra in the region from 90 GeV to 600 GeV. We completely confirm 'ATIC's excess' measured in ATIC-2 in this region. At the energies lower than 90 GeV the energy dependent trigger of the ATIC apparatus becomes important and some correction procedure should be applied. We do not describe this procedure here, and it is yet clear that our procedure deviates in detail from the one used by [5]. Such deviation may explain the differences of the spectra at $E < 90 \text{ GeV}$. The statistics at $E > 600 \text{ GeV}$ is very low and besides one may expect high proton background that may depend on the details of the simulations for the electron filter used, as shown above. These circumstances easily may explain any deviation of our spectrum from the spectrum of [5] in the region $E > 600 \text{ GeV}$ (three last points in our spectrum).

Now we compare our data for the ATIC-2 flight

with recent results for the electron spectrum in the region from 20 GeV to 1 TeV measured by Fermi/LAT telescope [9]. Remind that in this approximate analysis we used the spectra of ATIC without correction for the scattering in the atmosphere. The comparison is shown in Fig. 4. The comparison of ATIC's results and the spectrum of Fermi/LAT shows no sign of disagreement between the experiments. Actually, the ATIC spectrum are shown without subtraction of proton background. It is most probable that at the energies 30–100 GeV this background is not high (about 0.1–0.2 of the whole measured flux of the electrons plus proton contamination), but above some hundreds of GeV the intensity of background is higher. The ATIC data agree with Fermi/LAT at the energies less than 100 GeV well and the deviation above 300 GeV may be related to unaccounted background. The only significant difference of the ATIC's spectra from the Fermi/LAT's one is a sharp valley near 250 GeV. But the absence of this feature in Fermi/LAT results may be explained by much lower energy resolution of Fermi/LAT relative to ATIC.

The energy resolution of the ATIC apparatus for electrons actually is very high. It was shown during the beam tests of ATIC in CERN that the resolution is about 2% [10]. So high resolution provides a principle possibility to look for systematic-independent features and effects of a new type in the electron spectrum measured by ATIC. If the characteristic energy scale of this features is much shorter than the characteristic length of the variation of the proton background then such features would be independent of systematics related to proton background and may be safely studied.

The electron spectra for ATIC-2 flight plotted with bin width 0.03 for decimal logarithm of energy give an indication that between 200 GeV and 600 GeV some structure (three valleys and three peaks) exists in ATIC-2 spectrum. One may think that this is only a play of

statistics. Since the preliminary spectrum measured by ATIC-4 in the same region seems to have the same structure, this is a 'hint' that there may be short-scale features of the electron spectrum. However, it is necessary to first complete the detailed ATIC-4 analysis and to study the conclusions may be made. This is one of our on-going tasks.

Our conclusion is the following. The main advantage of the ATIC experiment is very high resolution in the measured electron spectrum. A main limitation of ATIC, or any thin calorimeter experiment, is the estimation of the proton contamination in the electron spectrum. Therefore, it is desirable to improve the construction of the ATIC spectrometer to reduce the proton background and to measure the electron spectrum both with high resolution and with low proton background.

REFERENCES

- [1] T. G. Guzik, J.H. Adams Jr, H.S. Ahn et al. *Adv. Sp. Res.*, V.33 (2004), P.1763.
- [2] V. I. Zatsepin, J. H. Adams, H.S. Ahn et al. *Nucl. Instr. Meth. A*, V.524(2004), P.195.
- [3] A.D. Panov, V.I. Zatsepin, N.V. Sokolskaya et al. *Instruments and Experimental Techniques*, V.51 (2008), P.665.
- [4] J. Chang, J.H. Adams Jr, H.S. Ahn et al. *Adv. Sp. Res.*, V.42 (2008) P.431.;
- [5] J. Chang, J. H. Adams Jr, H. S. Ahn et al. *Nature*, V.456, P.362–365 (2008).
- [6] J. Chang, et al., This conference (2009).
- [7] G. Battistoni, S. Muraro, P.R. Sala et al., *Proceedings of the Hadronic Shower Simulation Workshop 2006, Fermilab 6–8 September 2006*, M. Albrow, R. Raja eds., AIP Conference Proceeding 896, 31-49, (2007); A. Fasso', A. Ferrari, J. Ranft, and P.R. Sala, "FLUKA: a multi-particle transport code" CERN-2005-10 (2005), INFN/TC_05/11, SLAC-R-773
- [8] S. Agostinelliae, J. Allison, K. Amako et al. *Nucl. Instr. Meth.*, V.A506, P.250–303 (2003).
- [9] A. A. Abdo, M. Ackermann, M. Ajello, et al. *arXiv:0905.0025 [astro-ph.HE]* (2009).
- [10] O. Ganel, J.H. Adams Jr,, H.S. Ahn, et al. *Nucl. Instr. Meth.* V.A552 (2005), P.409.